THE AMERICAN MINERALOGIST, VOL 49, MAY-JUNE, 1964

# CORRELATIONS BETWEEN INFRARED SPECTRUM AND CHEMICAL COMPOSITION OF MICA

W. VEDDER, *General Electric Research Laboratory, Schenectady, New York.*

ABSTRACT

The infrared absorption and reflection spectra of samples of natural muscovites and phlogopites have been obtained as a function of orientation of the sample and as a function of temperature. In order to interpret the gross features of these spectra, a correlation has been sought with the vibrational modes of the silicon-oxygen network. The influence of components of the mica structure other than the Si-O lattice is discussed and the conclusion is drawn that mixing between Si-O and other modes of motion occurs.

Considerable attention is given to the vibrational modes of the OH ions and it is shown that the complexity of the OH stretching region in phlogopites is primarily associated with the detailed chemical composition and structure of the octahedral layer. Orientation and OH stretching frequency of OH ions close to various octahedral layer defects are discussed.

## INTRODUCTION

It is easy to identify two principal mica groups: dioctahedral micas, of which muscovite is the most widely occurring species, and trioctahedral micas such as phlogopite and biotite. For instance, the angle of the optic axes will range from 55° to 75° in the first group, but values below 15° are characteristic for the second.

The characterization of micas within each of the two groups is not so simple and in many cases only possible by means of a complete chemical analysis. Until the employment of $x$-ray emission techniques, this was a rather laborious process.

Over the years there has been considerable effort to find alternative and easier means of identification. Such properties as density, hardness, strength and thermal stability, electrical properties as resistivity, dielectric constant, dielectric loss and dielectric strength, optical properties as refractive index, angle of optic axes, reflection and absorption give a sufficient description of the material for some practical purposes. However, from a fundamental point of view, one would like to know precisely what basic structures can occur in the mica family, to understand in detail how crystalline solutions are formed and to derive from this structural information the functional relationships between chemical composition and physical properties. Subsequently, one might hope that such knowledge would lead to a "practical, reproducible, scientific test to evaluate sheet mica for specific end uses," the need for which was stressed recently (Skow, 1960).

Although the basic structure of mica has been known for a long time (Pauling, 1930) only recently have accurate structure determinations

become available (Radoslovich, 1960; Steinfink, 1962). (For a summary of composition and structure of mica, see Vedder and McDonald, 1963.) These studies have added several important refinements to the structures proposed by Pauling.

Among these are the considerable trigonal distortion of the Si-O network, the indications that the Si-Al substitution is partly ordered in muscovite and probably random in phlogopite, and the detailed arrangement of oxygen and hydroxyl ions around the octahedral layer of muscovite.

Foster (1956, 1960) has made a systematic study of many chemical analyses of micas. The experimental error in these analyses and the difficulties of interpretation introduce considerable uncertainty in the final structural formulas. Nevertheless, it appears that some major conclusions are beyond any doubt. Naturally occurring "dioctahedral" micas (*e.g.*, muscovite, ideal composition $KAl_2Si_3AlO_{10}(OH)_2$), except for lithium containing species, are always truly dioctahedral. The maximum number of occupied octahedral sites appears to be 2.05 per 3 available sites. Trivalent ions may enter the octahedral layer of "trioctahedral" micas (*e.g.*, phlogopite; ideal composition $KMg_3Si_3AlO_{10}(OH)_2$) in two different ways: by a substitution of ion for ion or by the simultaneous creation of vacancies in the layer; or in other words, by maintaining either the population or the charge of the octahedral layer constant. In practice both processes occur but in varying ratios. Some natural "trioctahedral" micas show occupation of the octahedral layer considerably below 3 per 3. The larger deviations from 3 are generally found among the iron-rich micas. However, it appears to be well established that there is a limit to the number of vacancies that can be introduced in the octahedral layer. Foster (1960) has found no "trioctahedral" micas with an octahedral occupancy below 2.45 per 3 sites. Hence it follows from the study of natural samples that there is a break in the series of crystalline solutions between di- and trioctahedral micas. This conclusion appears to apply equally well to synthetic micas.

From among the properties listed earlier, the optical spectra, more in particular the infrared spectra, appear to hold considerable promise of adding to the understanding of layer silicate structures. Progress in this area has recently been reviewed by Van der Marel and Zwiers (1959), by Fripiat (1960), and by Stubican and Roy (1961a, 1961b).

In summary it may be said that:

a. The usefulness of infrared spectra for the identification of layer silicates has been amply documented. There is considerable difference between spectra of very similar compounds as is quite clearly shown for example in the work of Stubican and Roy (1961a) and Beutelspacher (1956).

b. Many of the prominent absorption bands in the spectra have been given an interpretation. Matossi (1949) was the first to pay attention to the common features of many silicate spectra and, correctly, associated these with the vibrational modes of the SiO network. Since then the vibrational analysis of the SiO networks has been considerably refined (Saksena, 1961; Stepanov and Prima, 1958; Prima, 1957; Spitzer and Kleinman, 1961; Kleinman and Spitzer, 1962) and bands have been correlated to other groups or bonds commonly occurring in layer silicates (summarized by Stubican and Roy (1961a, 1961b)).

c. There are still many features of the infrared spectra of which the interpretation, though incomplete, has sufficiently developed to indicate that there is correlation to very interesting aspects of the structure. A good example of this is the $3\mu$ region of the spectrum where absorption occurs due to the stretching motion of the OH groups. This absorption band has been used to determine the orientation of the OH ions[1] in muscovite (Tsuboi, 1950; Serratosa and Bradley, 1958; Sutherland, 1955; Vedder and McDonald, 1963). Differences in the $3\mu$ regions of the spectra of di- and trioctahedral layer silicates and in some cases also the fine structure of the OH stretching band have been shown to be correlated to the structure (Van der Marel and Zwiers, 1959; Fripiat, 1960).

Many of these previous studies were carried out with small crystals of natural or synthetic materials suspended in mulls or alkali halide pressed pellets. Particle size has been kept very small to minimize reflection effects. In films of small particles, deposited from a suspension, considerable preference for some particular orientation may occur and this made it possible to obtain qualitative information about pleochroism (Farmer, 1958; Serratosa *et al.* 1962). However, for quantitative studies of pleochroism fair-sized single crystals are necessary.

It is the purpose of this paper to discuss the anisotropy of absorption in the infrared spectra of single crystals of natural micas. The samples employed were not pure compounds in a chemical sense. Some of our results might be derived in a more straightforward way if pure (synthetic) specimens of some size were available.

## Experimental Procedures

Spectra have been recorded with a fore-prism-grating instrument from 4000 to 650 $cm^{-1}$ and with a CsBr prism instrument from 700 to 300 $cm^{-1}$. Under operating conditions the resolution was 6 $cm^{-1}$ or

[1] What is determined experimentally is actually the direction of the vibrational transition moment. This can be considered to be the resultant of an intrinsic vibrational moment along the OH bond and a moment induced in the environment. The latter does not necessarily have the same direction as the OH bond.

Alternatively one can state the problem in terms of the difference in magnitude and direction of macroscopic and effective electric fields in the solid (Polo and Wilson, 1955).

In simple cases the correction factor is about $(n^2+2)/3$ ($n$=refractive index). With no more than 10% anisotropy in refractive index and with $n$ about 1.5 the OH bond direction should not differ from the orientation of the transition moment by more than 3°.

better throughout the entire region. An AgCl polarizer was used from 4000 to 650 $cm^{-1}$, a polyethylene polarizer in the 700 to 300 $cm^{-1}$ region. Tilt experiments were carried out with the light polarized in the plane defined by the normal to the cleavage surface and the direction of incidence. For measurements at liquid nitrogen temperatures, the mica sheets were pressed between two KBr crystals to improve thermal contact. Measurements at high temperatures (up to 1000° C.) were carried

TABLE I. CHEMICAL COMPOSITION OF MICAS[1]

| | Brazilian muscovite | Madagascar amber | | Canadian amber | | |
|---|---|---|---|---|---|---|
| | | W#4 | W#12 | M#1 | W#13 | W#11 |
| $SiO_2$ | 44.4 | 39.0 | 37.8 | 40.1 | 40.4 | 37.2 |
| $Al_2O_3$ | 34.3 | 15.3 | 17.6 | 14.5 | 15.1 | 18.2 |
| $TiO_2$ | .28 | 1.48 | 1.13 | .74 | 1.43 | 1.24 |
| $Fe_2O_3$ | .92 | 1.29 | 1.20 | .03 | .24 | 1.44 |
| FeO | 1.29 | 6.6 | 3.55 | .28 | 1.71 | 4.46 |
| MgO | 1.56 | 20.3 | 23.9 | 27.8 | 26.6 | 22.7 |
| $Li_2O$ | .01 | .01 | .004 | .01 | .01 | .01 |
| CaO | .02 | .05 | .01 | .01 | .03 | .03 |
| $Na_2O$ | .75 | .16 | .26 | .52 | .35 | .29 |
| $K_2O$ | 10.8 | 11.0 | 10.9 | 10.4 | 10.7 | 10.9 |
| F | .07 | 2.8 | 1.29 | 2.51 | 3.07 | 1.25 |
| Ignition Loss | 4.26 | 3.87 | 4.30 | 4.19 | 4.94 | 4.07 |

[1] Analyses by Ledoux & Co., Teaneck, N. J.

out with an arrangement which chopped the light before entering the high temperature cell thus resulting in complete separation of transmitted light from emission of high temperature cell and sample.

## RESULTS

The results of chemical analyses of some of the micas used in this study are given in Table I. Table II shows the composition of the various layers calculated by the method that has been adopted by Foster, that is, assuming:

a. A cationic charge per unit cell of 44;
b. Only Si and Al in the tetrahedral layer and all tetrahedral positions occupied;
c. Ions like Al, Mg, $Fe^{3+}$, $Fe^{2+}$, Mn, Ti, and Li in the octahedral layer;
d. K, Na, Rb, Cs and Ca in the interlayer.

For many other phlogopites the total iron content and the titanium content were measured by *x*-ray spectroscopy.[1] The 5 phlogopite samples

[1] I am indebted to Mr. L. B. Bronk for carrying out these measurements.

TABLE II. STRUCTURAL FORMULAE OF MICAS

| | | Brazilian muscovite | Madagascar amber | | Canadian amber | | |
|---|---|---|---|---|---|---|---|
| | | | W#4 | W#12 | M#1 | W#13 | W#11 |
| Octahedral | Mg | .16 | 2.19 | 2.52 | 2.92 | 2.76 | 2.40 |
| | Al | 1.76 | .14 | .14 | .04 | .05 | .17 |
| | $Fe^{2+}$ | .07 | .40 | .21 | .02 | .10 | .27 |
| | $Fe^{3+}$ | .05 | .07 | .06 | .00 | .01 | .08 |
| | Ti | .01 | .08 | .06 | .04 | .08 | .07 |
| | Li | .00 | .00 | .00 | .00 | .00 | .00 |
| Tetrahedral | Si | 3.02 | 2.83 | 2.68 | 2.83 | 2.81 | 2.64 |
| | Al | .98 | 1.17 | 1.32 | 1.17 | 1.19 | 1.36 |
| Interlayer | K | .93 | 1.02 | .98 | .93 | .95 | .99 |
| | Na | .10 | .02 | .03 | .07 | .05 | .04 |
| | Ca | .00 | .00 | .00 | .00 | .00 | .00 |
| Octahedral population per three sites | | 2.06 | 2.88 | 3.00 | 3.02 | 2.99 | 2.98 |

TABLE III. OBSERVED FREQUENCIES

| Assignment (see text for details) | Phlogopite (M#1) **E** in cleavage plane | Muscovite (Brazilian) | |
|---|---|---|---|
| | | **E** in cleavage plane | **E** ⊥ cleavage plane |
| $3\nu_{OH}$ | | 10387 | |
| $2\nu_{OH}$ | ~7410 | 7088 | |
| | ~7324 | | |
| | 4457 | | |
| | 4371 sh | | |
| | 4303 | 4708 | |
| | 4204 | 4543 | |
| $\nu_{OH}$ + lower frequency modes | 4151 | 4260 | |
| | 4098 | 4200 | |
| | 3998 | 4106 | |
| | 3894 | 3874 | |
| | 3790 | | |
| | 3708 | | |
| | 3667 | 3650 sh | |

TABLE III—(*continued*)

| Assignment (see text for details) | Phlogopite (M#1) **E** in cleavage plane | Muscovite (Brazilian) | |
|---|---|---|---|
| | | **E** in cleavage plane | **E** ⊥ cleavage plane |
| $\nu_{OH}$ | 3625 | 3628 | |
| | 3600 | | |
| | ~3560 | | |
| | 3528 | | |
| | 3430 | 3444 | |
| $\nu_{OH}$– lower frequency modes | 3316 | 3308 | |
| | 3216 | 3117 | |
| | 3110 | 3003 | |
| | 2854 | 2707 | |
| | 2024 VW | 2045 VW | |
| | ~1800 VW | ~1800 VW | |
| | 1635 VW | | |
| | ~1000 VS | ~1070 sh, S | ~1120 W |
| Si-O stretching | ~ 963 VS | ~1024 VS | ~ 990 VS |
| | 905 sh, M | ~ 985 sh, S | ~ 930 VS |
| | | | 827 M |
| $\nu_{OH}$ libration | | 928 M | |
| | 804 W | | |
| | 773 W | 805 W | |
| | 728 W | 755 W | 756 W |
| | 708 W | 691 W | |
| | 658 W | 630 W | |
| | 607 W | | |
| Si-O bending | 497 sh, M | | |
| | 464 VS | 528 VS | 523 VS |
| | 445 VS | 472 VS | |
| $\nu_{OH}$ libration | | 408 M | |
| | 364 M | | |
| | 343 M | 351 M | |

of Table I provided a satisfactory calibration. The $Fe^{3+}$ concentration was estimated from the ultraviolet spectrum. This spectrum is very similar to that reported for ferric ion containing oxides by Wickersheim and Lefever (1962). The absorption bands at .9 and .7$\mu$ were therefore con-

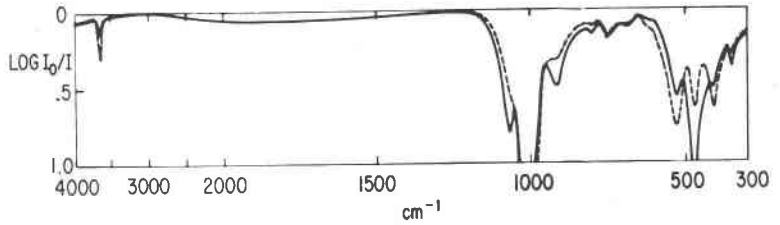


FIG. 1. Infrared absorption spectrum of Brazilian muscovite; d = 1.07$\mu$;
——— electric vector parallel to the *a* axis;
– – – – electric vector parallel to the *b* axis.

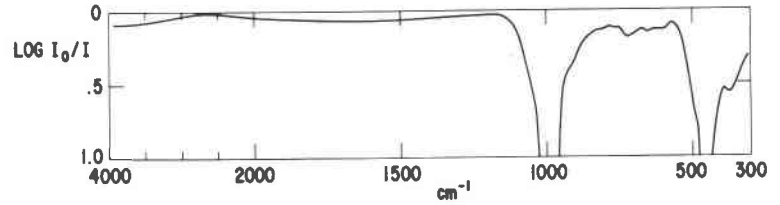


FIG. 2. Infrared absorption spectrum of a Canadian phlogopite (M#1); d = 1.28$\mu$; unpolarized light; electric vector in cleavage plane.

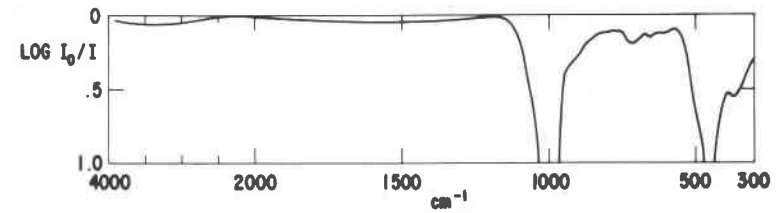


FIG. 3. Infrared absorption spectrum of a Madagascar amber (W#4); d = 1.36$\mu$; unpolarized light; electric vector in cleavage plane.

sidered part of the $^4G \leftarrow {}^6S$ transition in the crystal field modified spectrum of $Fe^{3+}$. Again by the use of the results in Table I, it was possible to calibrate U.V. intensity vs. $Fe^{3+}$ content. Neither of these methods is very accurate but the results are of considerable value for qualitative purposes.

In Figs. 1, 2, and 3 are shown the infrared absorption spectra of Brazilian muscovite, a nearly colorless Canadian phlogopite (M#1) and a dark brown phlogopite from Madagascar (W#4). The muscovite spectrum was obtained with light polarized along the *a* and *b* crystallographic

directions; in the case of the phlogopites, there is no anisotropy of absorption for the layer thicknesses used here and the spectra were taken with unpolarized light. Table III gives the observed frequencies.

It is not possible to prepare a single crystal layer parallel to the $c'$ axis[1] sufficiently thin to measure a useful absorption spectrum with $\mathbf{E}\|c'$. However, reflection spectra with light polarized parallel $a$, $b$, or $c'$ axes have been measured on optical surfaces $\|c'$ (obtained on a thick piece of Brazilian muscovite by ultrasonic abrasive cutting and polishing). The reflection spectra with $\mathbf{E}\|a$ or $\mathbf{E}\|b$ agreed perfectly with the corresponding spectra measured on cleavage surfaces.

These reflection data were subjected to a Kramers-Kronig transformation.[2] Each reflection curve was approximated by about 100 straight line segments. On the high frequency side the curves were assumed to approach a reflectivity equal to that calculated from the refractive index in the visible ($Na_D$) and to be constant from there on to higher frequencies. On the low frequency side the curves for $\mathbf{E}\|a$ and $\mathbf{E}\|b$ appear to converge satisfactorily toward the reflectivity calculated from the value of the dielectric constant at 10 Kc.[3] The reflection curve for $\mathbf{E}\|c'$ is at 300 $cm^{-1}$ lower than the reflectivity value which follows from the dielectric constant for $\mathbf{E}\|c'$ and it seems that there is another intense absorption band below 300 $cm^{-1}$ for $\mathbf{E}\|c'$. In order to permit the Kramers-Kronig transformation it was, rather arbitrarily, assumed that the reflectivity for $\mathbf{E}\|c'$ approaches 10% at 100 $cm^{-1}$ and is constant thereafter.

Figure 4 shows the reflection spectra of Brazilian muscovite with close to ($<6°$) perpendicular incidence and the light polarized parallel to $a$ or $b$ axes or perpendicular to $a$ and $b$ (parallel to $c'$). Figures 5 and 6 compare the measured quantity $t = -\ln T/d$ ($T$ = transmission, $d$ = thickness) with the absorption index $\epsilon$ calculated by Kramers-Kronig transformation from reflectivity data ($\epsilon = 4\pi k\tilde{\nu}$ with $\tilde{\nu}$ in wave numbers and k the imaginary part of the refractive index) for the cases $\mathbf{E}\|a$ and $\mathbf{E}\|b$.[4] Figure 7 shows the calculated absorption index with $\mathbf{E}\|c'$, for which no comparison with a measurement of t is available. However, the qualita-

[1] The direction perpendicular to the $a$ and $b$ axes is indicated as $c'$ axis. It deviates from the crystallographic $c$ axis by a few degrees.

[2] I gratefully acknowledge the cooperation of Miss E. L. Kreiger who carried out the calculation. A detailed description of the program for the Kramers-Kronig transformation has appeared as a technical report and is available on request from the authors (E. L. Kreiger, D. J. Olechna, D. S. Story).

[3] I am indebted to Dr. R. J. Charles for the measurements of the dielectric constant of Brazilian muscovite, parallel and perpendicular to the cleavage plane.

[4] t and $\epsilon$ are strictly not directly comparable; the transmission has not been corrected for reflection and interference effects.

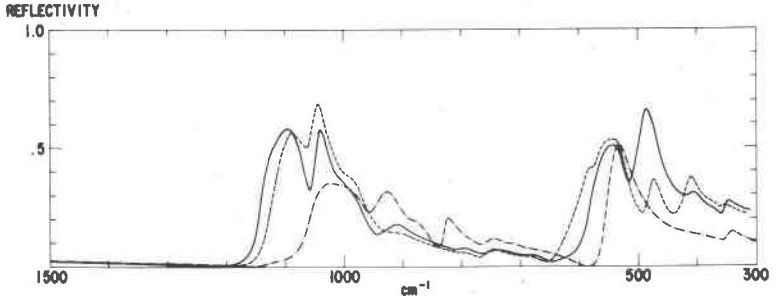


FIG. 4. Reflection spectra of Brazilian muscovite (close to perpendicular incidence);
——— electric vector parallel to the *a* axis;
– – – – electric vector parallel to the *b* axis;
–·–·–· electric vector perpendicular to the *a* and *b* axis.

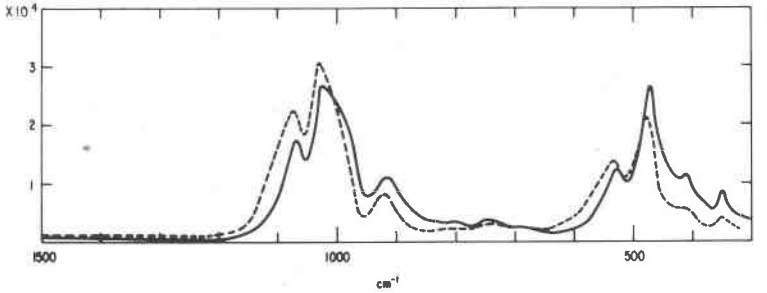


FIG. 5. Comparison of $t=-\ln T/d$ and $\epsilon=4\pi k/\lambda$ for muscovite (Brazilian) with $\mathbf{E}\|a$.

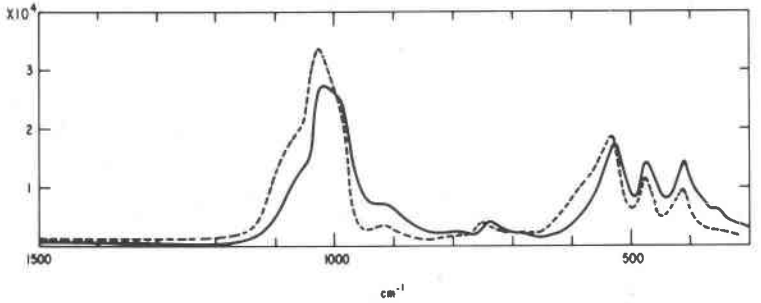


FIG. 6. Comparison of $t=-\ln T/d$ and $\epsilon=4\pi k/\lambda$ for muscovite (Brazilian) with $\mathbf{E}\|b$.

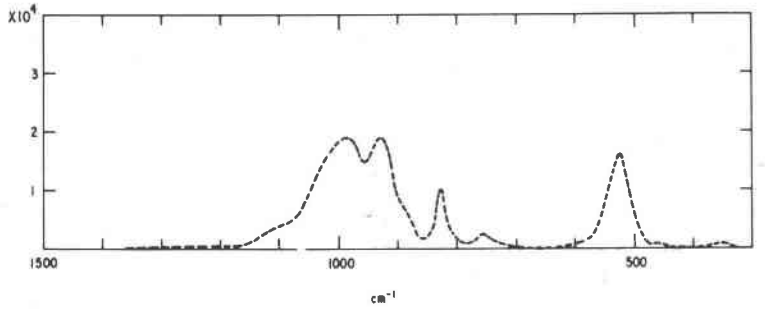


FIG. 7. $\epsilon = 4\pi k/\lambda$ for muscovite (Brazilian) with $\mathbf{E} \perp a$ and $b$.

tive agreement between measured t and calculated absorption index $\epsilon$ for $\mathbf{E} \| a$ and $\mathbf{E} \| b$ assures at least qualitative reliability for the calculated absorption spectrum with $\mathbf{E} \| c'$.

The OH stretching region is given in more detail in Figs. 8, 9 and 10 for the three micas. The Canadian phlogopite (M#1) is optically isotropic in the cleavage plane but in the case of muscovite and the Madagascar phlogopite (W#4) the spectra are shown with the light polarized along the $a$ and $b$ axes (which have different orientation with respect to a single layer for the $2M_1$ muscovite and, presumably, 1M phlogopite).

A larger frequency interval around the OH stretching frequency of the muscovite and the Canadian phlogopite at room and elevated temperatures is shown in Figs. 11 and 12. The highest temperatures at which spectra are shown are close to those at which decomposition of the mica begins to interfere.

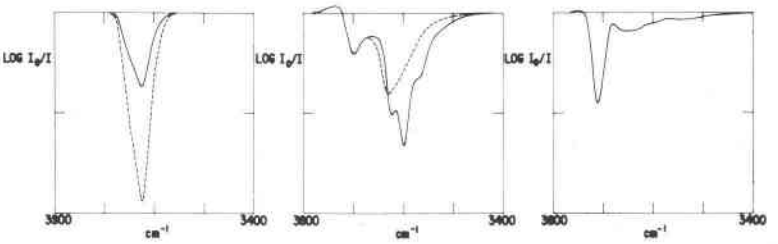


FIG. 8. (left) OH stretching region of infrared spectrum of Brazilian muscovite; d = 1.50$\mu$;
——— electric vector parallel to the $a$ axis;
– – – – electric vector parallel to the $b$ axis.

FIG. 9. (center) OH stretching region of infrared spectrum of Madagascar amber (W#4); d = 104$\mu$;
——— electric vector parallel to the $a$ axis;
– – – – electric vector parllel to the $b$ axis.

FIG. 10. (right) OH stretching region of infrared spectrum of a Canadian phlogopite (M#1); d = 110$\mu$; unpolarized light.

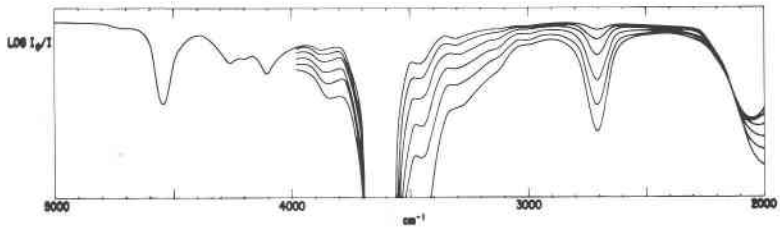


FIG. 11. Infrared spectrum of Brazilian muscovite around $\nu_{OH}$. Unpolarized light; d=325$\mu$; perpendicular incidence. Temperatures: 27°, 97°, 184°, 302°, 420° and 588° C.

The variation of the integrated intensity of the OH stretching band of muscovite with the direction of the electric vector of the light inside the crystal is shown in Fig. 13. Similar results for the phlogopite from Madagascar are shown in Fig. 14.

The 3$\mu$ spectra of various phlogopites and biotites are compared in Fig. 15; a spectrum of a fluorolube mull of talc is shown for comparison.

## SI-O NETWORK

All layer silicates are characterized by a (Si,Al)O network in the form of a sheet of interconnected tetrahedrons. It appears desirable, therefore, to carry out a vibrational analysis of such a network with the hope of creating a basis from which to start an assignment of observed vibrational frequencies. Such calculations for the SiO network in quartz, pioneered by Saksena (1961) since 1940, have recently been advanced by Kleinman (1962) and Spitzer (1961) to a point where experiment and theory appear very satisfactorily matched. Matossi (1949) has studied various other silicate structures but the vibrational analysis of a sheet

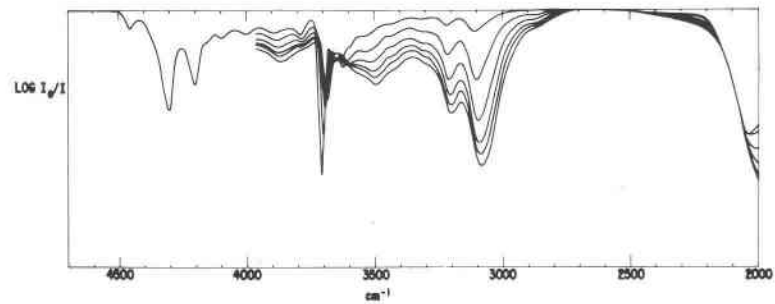


FIG. 12. Infrared spectrum of Canadian phlogopite (M#1) around $\nu_{OH}$. Unpolarized light; d=360$\mu$; perpendicular incidence. Temperatures: 27°, 279°, 482°, 620°, 722° and 796° C.

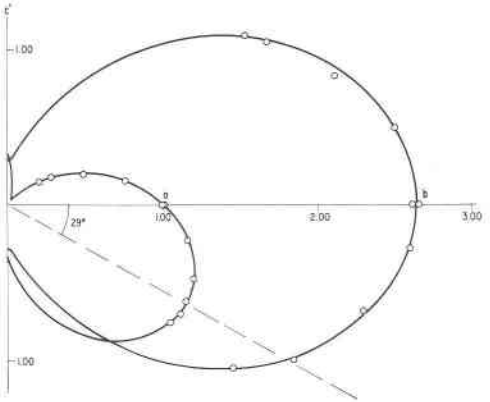


FIG. 13. Variation of integrated intensity of $\nu_{OH}$ of Brazilian muscovite with the orientation of the electric vector relative to the crystallographic axes.

structure has only recently been undertaken by Stepanov and Prima (1958), by Prima (1957) and by Saksena (1961). They have studied an arrangement of $SiO_4$ tetrahedrons as shown in Fig. 16. Saksena used a valence force field with two SiO stretching force constants (different values for the $Si\text{-}O_{bridged}$ and $Si\text{-}O_{non-bridged}$ stretching) and a force constant for the O-Si-O bending. Stepanov and Prima have used an additional

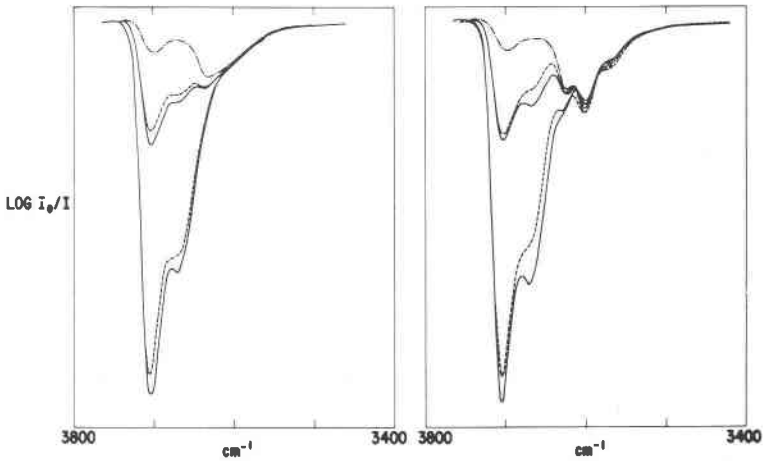


a. b.

FIG. 14. Variation of intensity of $\nu_{OH}$ in Madagascar amber (W#4) with orientation. Perpendicular incidence, $\pm 20°$ and $\pm 40°$ tilt. Polarized light;

a. electric vector in $b$-$c'$ plane,

b. electric vector in $a$-$c'$ plane.

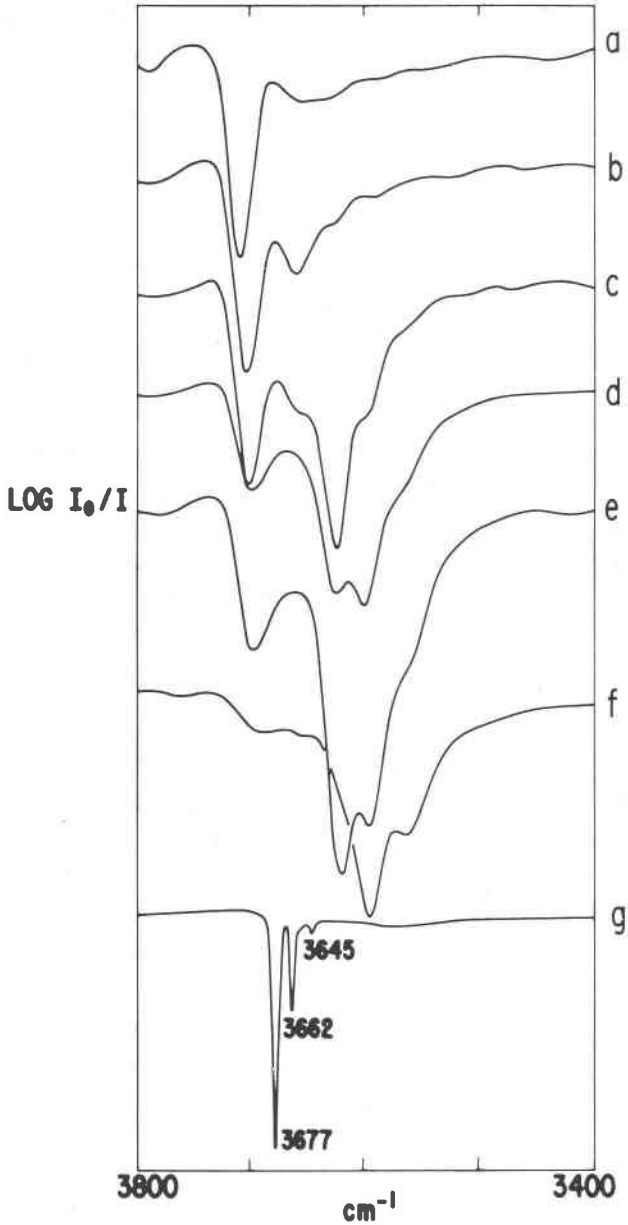


FIG. 15. OH stretching vibration in various phlogopites and talc. From top to bottom:
a. Canadian phlogopite; d = 100$\mu$; total iron content from $x$-ray spectroscopy .01[5]/3,
b. Madagascar amber; d = 100$\mu$; total iron content .30/3,
c. Canadian amber; d = 100$\mu$; total iron content .34/3,
d. Madagascar amber; d = 100$\mu$; total iron content .50/3,
e. Biotite; d = 100$\mu$; total iron content .62/3,
f. Biotite; d = 10$\mu$; total iron content. .76/3,
g. Talc (Eden, N. H.); fluorolube mull: total iron content .32/3.

bending force constant (Si-O-Si). This still falls considerably short of a complete valence force field because a force constant for torsion of the $Si\text{-}O_{bridged}$ bond and various off-diagonal terms would have to be added. In our own normal coordinate analysis, we have included the torsion force constant. Apart from this, our final equations are identical with those obtained by Prima (1957). There are differences with the equations obtained by Saksena (1961).

It is doubtful whether further refinements in the force field are desir-

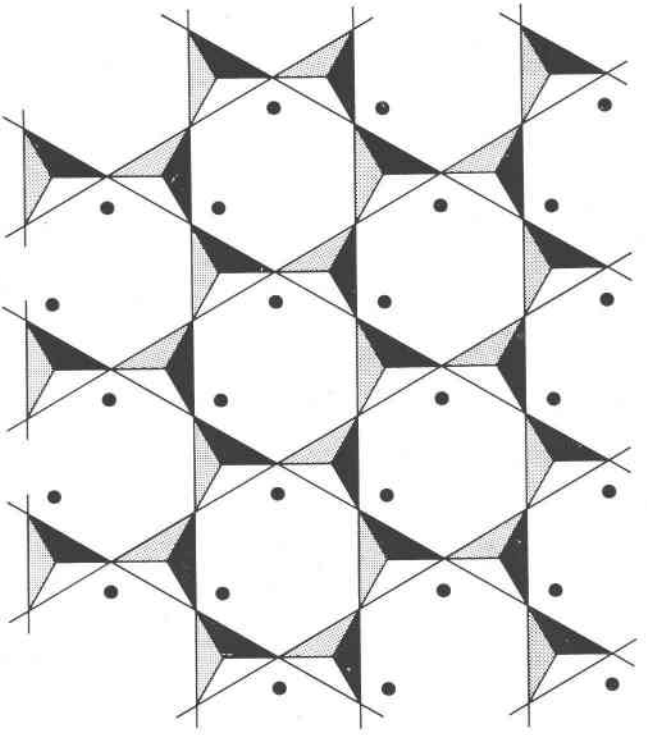

FIG. 16. Hexagonal network of $SiO_4$ tetrahedons. The dots indicate the positions of aluminum ions in the neighboring octahedral layer in the case of muscovite.

able as long as the analysis pertains to part of the crystal lattice only. As a result of the environment of the SiO sheet there may be contributions to the force field which cannot be properly accounted for by a valence force field. In addition it has to be expected that the environment will not remain rigid during vibrations of the sheet which at best necessitates substitution of the masses of Si and O atoms by unknown "effective" masses.

Finally, the arrangement of $SiO_4$ tetrahedrons in the crystal deviates considerably from the hexagonal network of Fig. 16.

Summarizing, it has to be expected that it may not be possible to match the experimental frequencies satisfactorily with a small set of valence force constants and the actual masses of silicon and oxygen; frequencies as well as selection rules will have to be corrected for the distortion from hexagonal symmetry.

For a SiO network of hexagonal symmetry (two dimensional unit cell group $C_{6v}$; $SiO_4$ on site $C_{3v}$) as shown in Fig. 16 vibrational modes of the following symmetry species are expected:

$$2A_1 + 3B_1 + B_2 + 3E_1 + 3E_2$$

Of these the $A_1$ modes are infrared active with transition moments parallel to $c'$, the $E_1$ modes are active perpendicular to $c'$. All other species are inactive.

As shown by Radoslovich (1960) for muscovite and Steinfink (1962) for phlogopite, the sheet is actually more like that shown in Fig. 17 in which each tetrahedron has been rotated about the $Si\text{-}O_{non\text{-}bridged}$ axis, half of them clockwise, the other half counter-clockwise (magnitude of rotation $10 \pm 4°$) (Radoslovich and Norrish, 1962). The symmetry of the two dimensional unit cell has been reduced to $C_{3v}$ with the $SiO_4$ groups on site $C_3$. As a result the $B_1$ modes remain inactive but the $B_2$ mode, which is closely associated with the motion leading from the hexagonal to the trigonal arrangement, becomes infrared active, polarized $\| c'$. Also the $E_2$ modes become active, polarized $\perp c'$.

The final arrangement of the sheet in the crystal leaves essentially only one symmetry element intact, namely, a plane parallel to $c'$ and crossing the sheet along the arrow in Fig. 17. At this point all modes become active and the degeneracy of the E modes is lifted.

Table IV compares force constants of quartz and zircon with values that have been proposed to account for a number of other silicate structures. The agreement in magnitude of the stretching force constants of the $SiO_4$ tetrahedron is fair but the situation regarding the bending force constants is much less satisfactory.

It is instructive to consider in some detail the vibrational modes of the silicate sheet for the case that each atom is constrained to move parallel to $c'$ only. The analysis predicts $2A_1+2B_1+E_2$ vibrational modes. The $2A_1+2B_1$ modes can be visualized as related to the two stretching vibrations of a linear triatomic molecule $[O_3]$-Si-O; in the $A_1$ modes the two tetrahedrons per unit cell vibrate in phase whereas in the $B_1$ modes they move out of phase.

When atoms are free to move in three dimensions and the symmetry is reduced it may be expected that there will remain an $A_1+B_1$ doublet

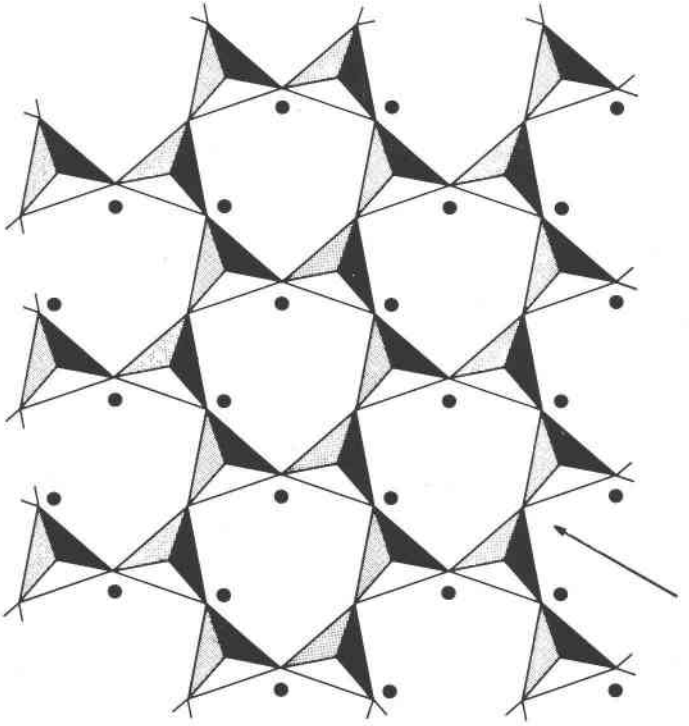

FIG. 17. Distorted network of $SiO_4$ tetrahedrons. The dots indicate the positions of aluminum ions in the neighboring octahedral layer in the case of muscovite.

TABLE IV. COMPARISON OF FORCE CONSTANTS ($10^5$ DYN/CM)

| | Quartz Kleinman-Spitzer (1962) | Zircon Matossi (1949) | Silicates in general | |
|---|---|---|---|---|
| | | | Saksena (1961) | Stepanov (1958) Prima (1957) |
| Stretching | | | | |
| $Si\text{-}O_{bridged}$ | 4.32 | — | 4.0 | 4.42 |
| $Si\text{-}O_{non\text{-}bridged}$ | — | 4.0 | 5.0 | 5.53 |
| Bending | | | | |
| O-Si-O | 0.24; 0.39 | .38 | .7 | .58 |
| Si-O-Si | 0.093; −0.33 | — | — | .17 |

which can still be approximately interpreted as stretching motion of O against (Si-[$O_3$]). There will also be a second doublet in which to a first approximation [$O_3$] moves against (Si-O), and which is a mixed stretching-bending mode. In each case the intensity of the $B_1$ component of the doublet should remain the lower of the two.

This qualitative assignment is reflected in the results of a calculation of frequencies for the case that only the SiO stretching force constants

TABLE V. COMPARISON OF CALCULATED AND EXPERIMENTAL FREQUENCIES

| Symmetry Species | Experimental Frequencies (Brazilian Muscovite) | Calculated frequencies | |
|---|---|---|---|
| | | f=3.89 $10^5$ dyn/cm F=4.68 $10^5$ dyn/cm | f=3.80 $10^5$ dyn/cm F=4.60 $10^5$ dyn/cm b=.37 $10^5$ dyn/cm |
| $A_1$ | 522 | 368 | 554 |
| | 930 | 921 | 941 |
| $B_1$ | — | 0 | 289 |
| | 826 | 812 | 818 |
| | 982 | 982 | 971 |
| $B_2$ | — | 0 | 0 |
| $E_1$ | — | 0 | 268 |
| | 498 | 0 | 482 |
| | 1020 | 1023 | 1041 |
| $E_2$ | — | 0 | 0 |
| | — | 0 | 419 |
| | — | 638 | 697 |

are given non-zero values. Following the trend of Table IV, the Si-$O_{non-bridged}$ stretching force constant (F) is taken 25% larger than the Si-$O_{bridged}$ stretching force constant (f). With f=3.89 $10^5$ dyn/cm (and F=4.86 $10^5$ dyn/cm) the results of Table V are obtained. This f value is so chosen that the $E_1$ frequency comes close to matching the experimentally observed $E_1$ mode at 1020 $cm^{-1}$.

It is interesting to compare the observed frequencies with the frequencies calculated for the modes which may be expected to give rise to absorption bands with a transition moment parallel to $c'$. Apart from the low frequency mode at 368 $cm^{-1}$ (calc.) there is a one-to-one correspondence between calculated and experimental data. Indeed there appears to be a higher (930+982 $cm^{-1}$) and a lower frequency $A_1+B_1$ doublet

(522+826 $cm^{-1}$). The intensity ratio in the latter is as predicted ($B_1 < A_1$) but the ratio of intensities of the 930 and 982 $cm^{-1}$ components is contrary to expectations. However, within the range of what seem to be acceptable relative magnitudes of F and f ($F \leq 2f$) the assignment cannot be reversed. Also the introduction of bending force constants alters this situation little and it is assumed that the unexpected intensity ratio is a consequence of the environment of the SiO network.

Frequencies calculated with a non-zero O-Si-O bending force constant (b) are given in Table V. Little or no improvement of agreement between calculated and available experimental frequencies is obtained when non-zero values are assumed for the Si-O-Si bending or $Si\text{-}O_{bridged}$ torsion force constants. Comparison with Table IV shows that the final force constants are satisfactorily close to values for analogous bonds in quartz and zircon.

A vibrational analysis of part of a structure is of little value unless an estimate can be made of the consequences of adding the omitted components to the part considered. In particular the question might well be asked what sense it makes to associate an experimental frequency of the phlogopite spectrum ($\sim$500 $cm^{-1}$) with the Si-O bending mode of the model where it is known that brucite has vibrational frequencies in the same part of the spectrum.[1] It would appear that at least two infrared active absorption bands have to be expected around 500 $cm^{-1}$ corresponding to mixed Si-O and Mg-O vibrations.

Simple model calculations indeed support this view. The higher frequency mode corresponds to Si-O bending with the Mg ions moving *against* the oxygen atoms. The frequency is higher than would be the case without the presence of Mg ions and the same holds for the intensity: the respective contributions of oxygen and magnesium ions to the dipole moment derivative add. The lower frequency mode corresponds to Si-O bending with the Mg ions moving *with* the oxygen atoms. Little additional restoring forces are added beyond those of Si-O bending and the effective mass is considerably increased giving rise to a lower frequency. The intensity is decreased because the respective contributions of magnesium and oxygen ions to the dipole moment derivative are opposed. Motion of magnesium ions relative to oxygen atoms mixes considerably with Si-O bending but little with Si-O stretching, this being determined by the relative frequencies.

The absorption bands which have been correlated earlier to vibrational modes of the SiO network are the most intense bands in the spec-

[1] Brucite, $Mg(OH)_2$, has an infrared active mode at about 515 $cm^{-1}$, a Raman active one at about 445 $cm^{-1}$ both of which have been tentatively assigned as lattice modes (Mitra, 1962).

trum and presumably all correspond to the cases in which octahedral ion motion adds to force constants and intensities. There must be additional absorption bands at lower frequencies with lower intensity. The model calculations indicate that frequencies for these might be around 300 $cm^{-1}$. This region of the spectrum may therefore contain considerable additional information about the octahedral layer.[1]

Arguments similar to those just presented apply to the vibrations of the interlayer ion. The force constant of K-O motion will be smaller than that of Mg-O motion. Hence the modes in which potassium participates will be at still lower frequencies and mixing with modes of the SiO lattice is small.

Little can be said about translational motion of the OH ion. The force constants of the bonds between this ion and its environment are certainly smaller than those of the surrounding non-bridged oxygen atoms. It would nevertheless seem likely that motion of the non-bridged oxygens is also mixed to some extent with OH ion translation. There should be a mode which is primarily OH translational motion at lower frequencies but there is no evidence of this in the spectra above 350 $cm^{-1}$.

In conclusion it can be said that the effect of adding ions to the Si-O network will be:

a. Mixing of the motion of the Si-O network with motion of the added ions. Mixing will be least for Si-O stretching but may be considerable for Si-O bending. Neither force constants nor intensities can be considered characteristic of the Si-O network alone.
b. Additional infrared active modes at lower frequencies.

Whereas phlogopites are nearly uniaxial, muscovites are clearly biaxial in the visible and infrared spectrum. This shows itself in differences between the spectra with $\mathbf{E} \| a$ or $\mathbf{E} \| b$. Most pronounced is the difference around 500 $cm^{-1}$. The splitting between the two differently polarized components at 477 and 535 $cm^{-1}$ is a result of the lifting of degeneracy of a two-fold degenerate vibrational mode of the pseudo-hexagonal lattice.

Strictly speaking, even in phlogopite no degeneracies can exist. However, in that case local symmetry around a $SiO_4$ tetrahedron is not far from threefold and splitting is negligible. In muscovite, the arrangement of Al ions and vacancies in the octahedral layer introduces a considerable asymmetry in the local force field and splitting becomes observable. The non-bridged oxygens are closer to the octahedral layer than the bridged ones. It is therefore reasonable that the splitting is more pronounced in the degenerate mode which is primarily $Si\text{-}O_{non-bridged}$ bending motion than in the one which is primarily $Si\text{-}O_{bridged}$ stretching.

[1] In the region from 250 to 33 $cm^{-1}$ of the far infrared muscovites show absorption bands at 188, 165 and 109 $cm^{-1}$. Of these the first shows the strongest dichroism whereas the last is the most intensive. Phlogopites have absorption bands at 151 and 86 $cm^{-1}$. I am grateful to Dr. S. Roberts for these measurements.

With this assignment, the doublet structure in the SiO bending region becomes one of the most characteristic features of a *di*octahedral layer silicate. *Both* components involve mixed Si-O bending and octahedral cation motion; the splitting is associated with the arrangement of occupied and unoccupied positions in the octahedral layer. The spectra of some clay minerals are in agreement with this. Stubican and Roy (1961b) observed that the doublet changes from 540 and 478 $cm^{-1}$ to 490 and 432 $cm^{-1}$ in going from beidellite to nontronite, shifting both components with small change in splitting.

### OH Ions Stretching Motion

The stretching vibration of OH ions in muscovite, $\nu_{OH}$, occurs at 3628 $cm^{-1}$. The orientation of the transition moment has been derived from anisotropy of absorption (Vedder and McDonald, 1963) and is found to be at an angle of 16° with the cleavage plane, away from the octahedral layer, with the projection onto the cleavage plane at 32° with the *b* axis. The OH ions themselves are probably oriented with nearly the same azimuth and with a latitude which exceeds 16° by at most a few degrees. Interpreted in terms of a point charge model, the intensity of $\nu_{OH}$ leads to about .25 of an electron charge on the proton.

In phlogopites the $\nu_{OH}$ intensity is very low in spectra recorded with the beam perpendicular to the cleavage plane. This has been interpreted (Serratosa and Bradley, 1958) as a result of the fact that in this case the OH ions are oriented parallel to $c'$. Indeed, the intensity increases rapidly when the sample is tilted. It has also been pointed out that in spectra of lepidolite there are two absorption bands, one of which remains constant upon tilting and another which behaves like $\nu_{OH}$ in phlogopite. A doublet with similar characteristics was reported by Bassett (1960) in the spectrum of biotite and some phlogopites.[1] In another sample, kaolinite (Serratosa *et al.* 1962), the complexity is even greater showing four components of which three are sensitive to tilting and one is not.

A similarly complex spectrum is shown by some phlogopites as indicated in Figs. 9, 10 and 15. There are five components at about 3700, 3665, 3620, 3600 and 3565 $cm^{-1}$. Of these the ones at 3700 and 3665 $cm^{-1}$ (to which we will refer later as respectively the N and the I bands[2]) are strongly sensitive to tilting. The components at 3620, 3600 and 3565 $cm^{-1}$ (which we will call the V bands) are nearly independent of the angle between beam direction and $c'$ axis. The intensity of the V bands relative to the band at 3700 $cm^{-1}$ varies tremendously from one trioctahedral mica to another. The V bands are the major feature in the biotite spectrum.

[1] Bassett (1960) was the first to recognize the connection between the fine structure in the 3$\mu$ region and the structural and chemical arrangement of the octahedral layer.

[2] For the meaning of the abbreviations N, I and V, see Table VI.

Because of the different properties of these band systems it seems appropriate to discuss them separately.

*N and I bands.* The anisotropy of absorption in the $\nu_{OH}$ region has been studied on the sample of Canadian phlogopite (M#1) by means of tilting.

The data were interpreted in terms of a model in which all OH ions have the same colatitude (with respect to the $c'$ axis) and have a distribution of azimuths of at least three-fold symmetry. For this model it follows:

$$\text{Intensity} = A_0 \frac{\sin^2\phi + 1/2 \tan^2\delta \cos^2\phi}{1 + \tan^2\delta} \tag{1}$$

in which $A_0$ is the intensity if all OH ions were exactly parallel and the light polarized parallel to this OH direction; $\phi$ is the angle between the electric vector and the cleavage plane and $\delta$ is the colatitude of the OH ions with respect to the $c'$ axis (the incident light is assumed to be a parallel beam and to be polarized in the plane of the beam direction and the $c'$ axis).

Because the two components overlap little at the peak frequencies it seems convenient to use peak intensities to determine $\delta$. However, the peak of the 3708 component appears to shift to 3715 $cm^{-1}$ in the spectrum of the 40° tilted sample and the second component behaves similarly. The reason for this is that the (small) variation of the refractive index in the absorption region causes $\phi$ to be larger at the high frequency side, smaller on the low frequency side, with the result that the band appears to shift to higher frequencies when the tilt angle, and consequently the fluctuation in $n$, increases.

We have therefore not measured the intensity at the peak frequency for each tilt angle but at two fixed frequencies, equal to the peak frequencies at normal incidence. For each of the two components this leads to the value $\delta \simeq 11.5°$.

*V bands.* In order that the intensity of absorption be "$\phi$ independent" equation (1) requires $\delta \simeq 55°$. However, it is evident, for example from Fig. 9, that the intensity and shape of this group of bands depends on whether **E** is parallel to the $a$ or $b$ axis. With $\mathbf{E} \| a$ there are three clearly distinguishable components at 3622, 3600 and 3564 $cm^{-1}$. Whereas with $\mathbf{E} \| b$ there is a maximum at about 3630 $cm^{-1}$ tailing off gradually towards lower frequencies. The absorption in this region is also more intense (in the sample of Fig. 9 by a factor of 1.65) with $\mathbf{E} \| a$ than with $\mathbf{E} \| b$. If the model leading to equation (1) is modified to allow for anisotropy in azimuth "$\phi$ independence" requires $\delta$ to be close to 59° (see below).

It is safe to conclude, therefore, that the OH ions represented by this

group of absorption bands are oriented at an angle of the order of 60° with the $c'$ axis and are not randomly distributed in aximuth. The intensity of this group relative to the N-I doublet varies strongly between samples and there is also considerable variation in the relative intensities of the individual components of the group (Fig. 15).

A tentative assignment of the fine structure in the OH stretching region can be stated in terms of the occupation of the octahedral sites close to an OH ion, the three immediately neighboring sites playing a dominant role (Table VI).

TABLE VI

| | |
|---|---|
| N-band (normal) | OH ions for which the immediately neighboring octahedral sites are all filled with divalent ions; |
| I-band (impurity) | OH ions for which all three closest octahedral sites are occupied, one however by a trivalent ion (*e.g.*, $Fe^{3+}$ or Al) |
| V-bands (vacancy) | OH ions close to an unoccupied octahedral site. |

This assignment is supported by the following arguments.

*N-bands.* In talc of composition $KMg_3Si_4O_{10}(OH)_2$, characterized by complete occupancy of the octahedral layer by Mg ions and only Si in the tetrahedral sites, the OH ions are expected to be oriented exactly perpendicularly to the layer. All OH ions are equivalent, hydrogen bonding and coupling are small and one sharp OH stretching band may be expected. The spectrum of the talc sample in Fig. 15 shows *three* sharp bands at 3677, 3662, and 3645 $cm^{-1}$. In talcs the major impurity in the octahedral layer is $Fe^{2+}$. These bands are therefore interpreted as due to OH ions with the three closest octahedral sites occupied by respectively 3 Mg, 2 Mg+$Fe^{2+}$ and Mg+2 $Fe^{2+}$. For a random distribution of Mg and $Fe^{2+}$ in concentrations of respectively $1-X$ and X, it follows that the intensity ratio of these bands should be

$$1:3\,\frac{X}{1-X}:3\left(\frac{X}{1-X}\right)^2.$$

The experimental ratio of peak intensities is 1: .404: .061 which is about equal to the ratios calculated with $X=.119$. This value is acceptably close to $X=.107$ which is the concentration of total Fe estimated from $x$-ray spectroscopy using the phlogopite calibration. As is to be expected for a small perturbation, the shift of $\nu_{OH}$ for two $Fe^{2+}$ is very nearly twice that for one $Fe^{2+}$. It is concluded that:

a. Substitution of Mg by $Fe^{2+}$ shifts $\nu_{OH}$ by about 16 $cm^{-1}$ and cannot explain the fine structure observed in phlogopites.

b. Each of the components is still a sharp band ($\Delta\nu_{1/2} \simeq 5$ cm$^{-1}$). The presence of $Fe^{2+}$ cannot explain the considerable ($\Delta\nu_{1/2} \simeq 25$ cm$^{-1}$) width of the components in the mica spectrum.

It also does not seem very probable that $Fe^{2+}$ ions in the octahedral layer would tilt the OH ions by as much as 11.5°. The deviation from perpendicular orientation and the width of the absorption band appear to be associated with substitution of Si by Al in the tetrahedral layer. This assumption is not inconsistent with predictions on basis of a point charge model in which the position of the oxygen atom of the OH ions is assumed fixed and the force on the proton resulting from Si-Al substitution is balanced against restoring forces derived from the experimental librational frequency. Replacement of Si by Al can be considered equivalent to distributing one unit of negative charge in some way between the Si site and the four surrounding oxygens. The librational frequency is about 550 cm$^{-1}$. The force can be expressed as

$$\text{Force} = \frac{\delta}{\text{“}\epsilon\text{”}} \sum_i \frac{e_i}{r_i^2}$$

in which $\delta$ is the charge on the hydrogen atom and is taken equal to .5 which is the theoretical value (Clementi, 1962; Nesbet, 1962) of the "effective charge" on the proton for isoelectronic HF. A correction for the influence of the surrounding dielectric is applied by means of a formal dielectric constant "$\epsilon$" which is assumed equal to the dielectric constant of phlogopite, that is "$\epsilon$" $= 5.5 \pm .5$.

This calculation predicts that the OH ions are tilted by 8.1° if the whole unit of negative charge is put on the Si site. To allow for the fact that the Al-O bond is more ionic than the Si-O bond, a second case has been calculated, namely 40% of the unit of negative charge on the Si site and the remainder on the surrounding oxygens. This assumption predicts a tilt of 7.5°.

About one out of four Si is substituted by Al. If the Al ions were randomly distributed only the cases in which zero to three Al ions are among the six Si sites immediately surrounding an OH ion need to be considered. Repulsive interaction between the Al ions favors the cases of one Al or two Al with meta geometry (the distribution of Al over Si sites proposed by Radoslovich (1960) for muscovite is in a general way similar to the one described here). Assuming additivity it follows that the force on the proton by two Al ions in meta position relative to each other equals the effect of one Al ion; the maximum force (in the cleavage plane) by any number of Al ions neighboring an OH ion is twice that for one Al ion. The model predicts therefore a deviation of the OH orientation from perpendicular in the order of 0–15° with possibly considerable preference for angles of about 8°.

The difference between $\nu_{OH}$ in phlogopites ($\sim$3700 cm$^{-1}$) and muscovite ($\sim$3630 cm$^{-1}$) shows that frequencies are different when orientations are different.

It is concluded, therefore, that it is mainly the Si-Al substitution which is responsible both for the deviation from perpendicular orientation of the OH ions and the sizeable width of the OH stretching absorption band although other factors may also contribute. Increasing concentration of $Fe^{2+}$ ions displaces the N-band to lower frequencies.

*I-band.* Substitution of a divalent ion of the octahedral layer by a trivalent ion without the creation of a vacancy is generally balanced by a simultaneous substitution of Si by Al. The point charge model predicts that a closest neighbor trivalent ion should tilt an OH ion by about 6°. Whereas the forces on the proton from the Si-Al substitution are largely perpendicular to the OH direction, the force exerted by a trivalent ion in the octahedral layer contains a considerable component along the OH bond, stretching it and lowering the frequency. From the anharmonicity of the stretching motion ($\nu=\omega-2\omega x\simeq 3705$; $2\omega x\simeq 155$) the point charge model predicts $\Delta\nu=-11$ cm$^{-1}$ for the Si-Al substitution and $\Delta\nu=-34$ cm$^{-1}$ for a closest neighbor trivalent ion.

The model calculations are therefore not inconsistent with the assignment of the I-band to OH ions close to a trivalent ion in a completely filled octahedral layer.

This assignment is tested quantitatively against data derived from chemical analyses in Fig. 18. The observed ratio of peak intensities of the I and the N band is plotted against the theoretical ratio 3 X/Y in which X and Y are the fractions of octahedral sites occupied by respectively tri- and divalent ions as calculated in Table II (black circles). In order to estimate the quantitative significance of this comparison, the theoretical ratio of peak intensities is also calculated for the case that all titanium is assumed to replace silicon in the tetrahedral layer[1] (triangles) and the experimental ratio is corrected for the fact that the I-band is overlapped to some extent by the N-band and the first of the V-bands ($\sim$10% of their intensity at the peak of the I-band; open circles).

The rectangles in Fig. 18 are a measure of the uncertainties of this comparison and it is evident that these few data do not establish a quantitative relationship. Nevertheless it appears that the assignment given is essentially correct.

*V-bands.* The OH ions close to a vacant octahedral site will be tilted toward the vacancy by a considerable angle. The vacancy results in local

[1] There are indications that in some cases titanium is tetrahedrally coordinated (Serdyuchenko, 1948; Tarte, 1961).

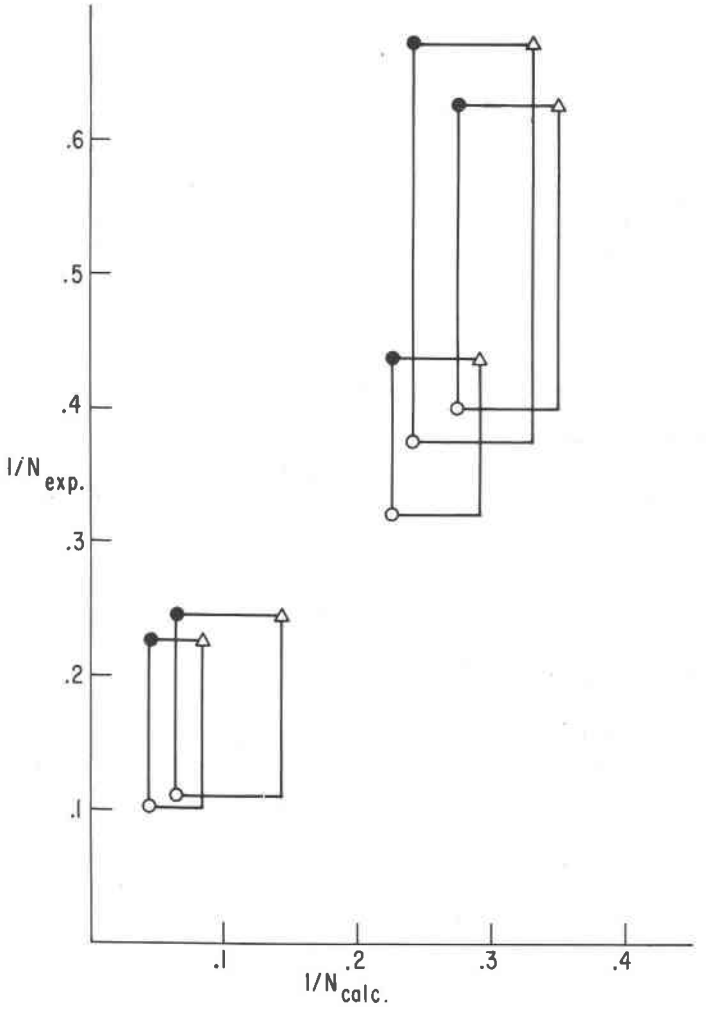


FIG. 18. Comparison of experimental ratio of peak intensities of the N- and I-bands with values calculated on basis of the assignment in Table VI;

● observed ratio of peak intensities and calculated ratio on basis of data in Table II;

△ observed ratio of peak intensities and calculated ratio assuming all titanium in the tetrahedral layer;

○ observed ratio corrected for band overlap; calculated ratio on basis of data in Table II.

distortion of the lattice (see muscovite structure (Radoslovich, 1960)), and for large deviations from perpendicular orientation it is impossible to assume a Hooke's law restoring force; model calculations have therefore become difficult to perform. However, the orientation of the OH ions

giving rise to the V-bands, as estimated from the aniostropy of absorption, is comparable to the orientation of OH ions in muscovite, all of which are close to a vacancy.

As has been pointed out, equation (1) does not apply to cases for which the distribution of azimuths of the OH ions has less than threefold symmetry. For the analysis of the V-bands, a model has been chosen which considers the three closest octahedral sites only and assumes that the angle by which the OH ion is tilted toward the vacancy is not dependent on which of the three sites is vacant. As a result of the symmetry of the layer, two of the octahedral sites, $A_1$ and $A_2$, are equivalent and related by a center of inversion; the third site, B, is the one which is unoccupied in the muscovite structure. The model supposes that the numbers of vacancies occurring on A or B sites are not necessarily equal.

The data of the sample of Madagascar amber (W#4) when fitted to this model indicate that 10% of the OH ions are near vacancies; of these about half are near a vacancy on an A site, the remainder near a vacancy on a B site. This means that in this phlogopite octahedral occupancy is 2.90 per 3 sites (from Table II follows 2.88 per 3 sites) and that vacancies have a preference for those sites which are completely unoccupied in the muscovite structure.

It is difficult to arrive unambiguously at an assignment for the three individual components. The most reasonable hypothesis seems that they correspond to the cases:

$\sim$3625 $cm^{-1}$; OH ions close to a vacancy + two divalent ions;
$\sim$3600 $cm^{-1}$; OH ions close to a vacancy + a divalent + a trivalent ion;
$\sim$3560 $cm^{-1}$; OH ions close to a vacancy + two trivalent ions.

In order to evaluate this assignment quantitatively, consideration has to be given to the fact that electrostatic calculation of the "bonding energy" of associations of vacancies and trivalent ions leads to values on the order of 1 eV. In view of the relatively low temperature of formation of phlogopites and of the sizeable concentration of trivalent ions in the samples in which vacancies occur, it seems reasonable to assume that nearly every vacancy is closely associated with trivalent ions. The existance of such association is also indicated by the two phase region in the phase diagram of di- and trioctahedral micas.

Assuming that it is appropriate to use electrostatically calculated energies as a guide[1] it may be expected that among the three possible configurations of the association $R^{3+}$-vacancy-$R^{3+}$, the ones with a "bond

[1] The interaction between a divalent cation and a sodium ion vacancy in NaCl is experimentally about .35 eV for $Cd^{2+}$ (Lidiard, 1954). Theoretical calculations give essentially the same value (Bassani and Fumi, 1954). The simple electrostatic model predicts .59 eV.

angle" of 180° or 120° are close enough in energy to occur with comparable probability. The association with "bond angle" 60° requires considerably more energy and should occur less frequently. More energy still would be required to dissociate these associations of two trivalent ions and a vacancy into a pair $R^{3+}$-vacancy and an isolated $R^{3+}$ ion. All of these defect associations can be stabilized to some extent by suitably chosen substitution between Si and Al. In the last case an Al could be substituted by Si near the pair $R^{3+}$-vacancy, the reverse being done near the isolated $R^{3+}$ ion.

Assuming that there is no strong preference for the *orientation* of an association in the octahedral layer, the intensities of the three bands are predicted as follows:

| Type Defect | Relative Intensities | | |
|---|---|---|---|
| | ~3625 $cm^{-1}$ | ~3600 $cm^{-1}$ | ~3560 $cm^{-1}$ |
| $R^{3+}$-vacancy (plus the additional processes required for neutrality) | 4/6 | 2/6 | 0 |
| $R^{3+}$——$R^{3+}$ \ 60° / vacancy | 3/6 | 2/6 | 1/6 |
| $R^{3+}$-vacancy-$R^{3+}$ with "bond angles" of 180° or 120° | 2/6 | 4/6 | 0 |

For higher vacancy concentrations, such associations will get close to one another and the intensity should shift entirely to the 3600 and 3560 $cm^{-1}$ bands.

From the observed intensitities in Fig. 15, it appears that some micas come close to representing one of the above cases. However, the available experimental data are too few to permit more than the conclusion that the assignment suggested for the individual components in the V-band system is reasonable but speculative. The conclusion that these bands are associated with the OH ions close to octahedral vacancies seems well established, however.

## OH Ions Librational Motion

Two librational modes have been identified in muscovite at frequencies 925 and 405 $cm^{-1}$, corresponding respectively to the motion of the OH ion such that the proton remains parallel to the cleavage plane or moves toward and away from it (Vedder and McDonald, 1963).

Attempts to deuterate phlogopite under conditions similar to those used for muscovite were unsuccessful and direct evidence of librational modes has not been obtained in this case.

*Combination bands with* $\nu_{OH}$. In muscovite and phlogopite, a large number of weak absorption bands occur on either side of $\nu_{OH}$. These are interpreted as combination bands involving the OH stretching mode and some other lower frequency mode.[1] It has been proposed that such spectra are associated with stretching and libration of the OH ions only (Hexter, 1961, 1963). Alternatively it has been pointed out that other modes than libration of the OH ions may combine with $\nu_{OH}$ (Wickerscheim, 1959; Buchanan and Caspers, 1963; Buchanan *et al.* 1962; Mitra, 1962).

Most hydroxide spectra are highly complex around $\nu_{OH}$ and in no case yet has an entirely satisfactory interpretation been possible. In this respect muscovite and phlogopite are no exception.

In the muscovite spectrum, the librational mode with frequency 925 $cm^{-1}$ occurs with considerable intensity in combinations with $\nu_{OH}$, both as a sum and a difference band. It should be noted that the intensity of these bands is nevertheless smaller than that of $\nu_{OH}$ itself by more than two others of magnitude. The difference band grows in intensity with temperature as expected for a transition from a level $860 \pm 50$ $cm^{-1}$ above the librational ground state. The corresponding sum band is practically independent of temperature. The ratio of the intensities of the difference and sum band is to a first approximation expected to be determined only by the population of their respective initial states. The observed ratio is larger than the expected Boltzmann ratio by a factor of $6 \pm .5$. This anomaly resembles the discrepancies between observed and calculated ratios of corresponding line intensities in P and R branches of vibration-rotation spectra. In that case, the effect has been shown (Herman and Wallis, 1955; Herman and Rubin, 1955) to be due to Coriolis interaction between vibration and rotation. Any mixing of stretching and libration in our case could lead to similar deviations from Boltzmann ratios. Cross terms involving stretching and libration coordinates may be expected to occur in potential and dipole moment expansions whenever the equilibrium OH distance is a function of orientation of the OH ion and this is undoubtedly the case.

Fairly intense combinations occur which seem to involve modes with frequencies from 480 to 640 $cm^{-1}$; no sum or difference band is observed

[1] In the course of this discussion it will become clear that I consider the interpretation of the OH region in terms of OH stretching motion plus combinations of this motion with lower frequency modes to be essentially correct. I, therefore, disagree with the views of Boutin and Bassett (1963).

with $\nu_{OH}$ and the librational frequency at 405 $cm^{-1}$. The conclusion seems inevitable that other than librational modes take part in combination bands. Some of these other modes do not appear as infrared active fundamentals although all are close in frequency to strongly active modes. In this connection, it is interesting to note that there is evidence of a sum band with the mode at 1083 $cm^{-1}$, but none with the strongly active Si-O stretching mode at 1020 $cm^{-1}$. It seems that combinations occur more readily with Si-O bending than with Si-O stretching modes. This may not be surprising when looked at from the point of view that intensities are determined by the magnitude of cross terms in potential energy and dipole moment expansions.

$\nu_{OH}$ itself shifts from 3628 $cm^{-1}$ at room temperature to about 3617 $cm^{-1}$ at 530° C. The peak intensity decreases slowly with increasing temperature but the dichroic ratio,

$$\frac{\text{intensity for } \mathbf{E}\|b}{\text{intensity for } \mathbf{E}\|a},$$

remains constant within experimental accuracy.

One of the most interesting features of the phlogopite spectrum as a function of increasing temperature (below 600° C.) is the rapidly decreasing intensity of the fundamental stretching frequency (N-band). This is a clear indication that the intensity with which $\nu_{OH}$ is observed at perpendicular incidence is not associated with thermal motion (nor all due to the use of convergent light in the spectrometer or misalignment of the sample). Instead, it is associated with the deviation from perpendicular orientation of the OH ions, although it is not immediately clear why there should be a decrease in intensity with increasing temperature.

Also in the phlogopite case $\nu_{OH}$ shifts to lower frequencies with increasing temperature; from about 3708 at room temperature to 3684 $cm^{-1}$ at 796° C (M 1).

Again many sum and difference bands are observed. They appear to be more symmetrically spaced around $\nu_{OH}$ than in the case of muscovite. Most intense among them are two doublets, one of which can be represented as $\nu_{OH}+$(496 and 595), the other as $\nu_{OH}-$(492 and 598). It is expected that these doublets are in some way associated with librational motion. However, considering the complexity of the muscovite spectrum in the regions where combinations of $\nu_{OH}$ and the 405 $cm^{-1}$ libration were expected to occur, it is impossible to say whether in this case the doubling is due to two components of librational motion or interference with modes of different origin. If necessary, two librational frequencies could be accounted for by the small tilt from perpendicular orientation of the OH ions, the splitting 405–925 $cm^{-1}$ in muscovite being a further advanced example of this.

The temperature dependence of the intensity of the difference doublet indicates that they are transitions from levels roughly 600 $cm^{-1}$ above the ground state. Both components of the difference doublet are more intense than expected on basis of Boltzmann populations of their initial levels. The discrepancies are not so large as in the case of muscovite, however, and smaller for the $\nu_{OH} \pm 494$ components (factor about 1.5) than for the $\nu_{OH} \pm 597$ components (factor about 3).

In the muscovite and phlogopite spectra considerable changes appear at higher temperatures close to $\nu_{OH}(\pm 300\ cm^{-1})$. It has to be anticipated that in potential energy and dipole moment expansions, cross terms of some magnitude occur between the translational motion of the OH ion and its stretching. Combination modes and hot bands involving stretching and translation must therefore be expected. However, translational motion of the OH ion will be thoroughly mixed with other lattice modes and a discussion of this part of the spectrum is extremely difficult.

## Summary

Frequencies of the most intense bands of the mica spectrum are correlated with vibrational modes of a part of the mica structure, namely the Si-O layer lattice, using a valence force field with three force constants and the actual masses of oxygen and silicon. It is pointed out that this correlation is of limited significance because of considerable mixing of the motion of the Si-O layer and its environment. The qualitative effects of this mixing are discussed. The environment influences frequencies and intensities of the modes previously assigned to Si-O motion and gives rise to new absorption bands at lower frequencies. Consequently, it is not justified to interpret observed absorption bands in terms of Si-O motion only, particularly not in the Si-O bending region.

Compared to muscovite, phlogopites show a very complex system of bands in the OH stretching region. The stretching frequency is about 3700 $cm^{-1}$ for an OH ion with only divalent nearest neighbor octahedral ions (N-band) and 3660 $cm^{-1}$ for an OH ion with the three nearest neighbor octahedral positions occupied by two divalent and one trivalent ion (I-band). Both OH ions are nearly but not quite perpendicular to the layer plane. The Si-Al substitution in the tetrahedral layer contributes considerably to this small tilt.

Hydroxyl ions close to an unoccupied octahedral site give rise to a separate band system (V-bands) with quite different anisotropy of absorption indicating considerable tilting. There are three bands, at about 3620, 3600 and 3560 $cm^{-1}$, the frequencies of which have been tentatively correlated to the charge of the ions occupying the two remaining closest neighbor octahedral sites.

These assignments furnish a tool for the study of the detailed structure and chemical composition of the octahedral layer about which until now little direct information could be obtained. The results on the micas should be applicable to layer silicates in general.

Librational motion is discussed as it appears in fundamentals and in combination bands with the OH stretching mode. The intensity of the difference bands increases with temperature as expected but is in some cases too high relative to the corresponding sum bands by a factor as large as 6 (muscovite). The change of the equilibrium OH distance with orientation is tentatively held responsible for this.

## Acknowledgments

The author is grateful to Dr. R. S. McDonald and Dr. G. L. Gaines for their valuable interest during this study. Their helpful suggestions and comments during the preparation of this manuscript have led to considerable improvement.

Specimens of mica have been kindly put at the author's disposal by Drs. G. L. Gaines, W. L. Walton, L. Navias and R. C. deVries of the General Electric Company. A gift of Canadian phlogopites from Mr. M. S. Mead is gratefully acknowledged. A number of very interesting samples have been made available by the New York State Museum in Albany, New York. For this courtesy the author expresses his appreciation to Mr. R. L. Borst, associate curator of Geology.

## References

Bassani, F. and F. G. Fumi (1954) The association energy between positive divalent impurities and positive-ion vacancies in NaCl and KCl crystals. *Phil. Mag.* **45,** 228–230.

Bassett, W. A. (1960) Role of hydroxyl orientation in mica alteration. *Bull. Geol. Soc. Am.* **71,** 449–456.

Beutelspacher, H. (1956) *Landwirtschaftl. Forschung, Sonderheft* **7,** 74–79.

Boutin, H. and W. Bassett (1963) A comparison of OH motions in brucite and micas. *Am. Mineral.* **48,** 659–663.

Buchanan, R. A. and H. H. Caspers (1963) Answer to "Comment on infra-red absorption spectra of LiOH and LiOD." *Jour. Chem. Phys.* **38,** 1025–1026.

———, E. L. Kinsey and H. H. Caspers (1962) Infra-red absorption spectra of LiOH and LiOD. *Jour. Chem. Phys.* **36,** 2665–2675.

Clementi, E. (1962) SCF-MO wave functions for the HF molecule. *Jour. Chem. Phys.* **36,** 34–44.

Farmer, V. C. (1958) The infra-red spectra of talc, saponite, and hectorite. *Mineral. Mag.* **31,** 829–845.

Foster, M. D. (1956) Correlation of dioctahedral potassium micas on the basis of their charge relations. *U. S. Geol. Survey Bull.* **1036-D.**

——— (1960a) Layer charge relations in the dioctahedral and trioctahedral micas. *Am. Mineral.* **45,** 383–398.

——— (1960b) Interpretation of the composition of trioctadehral micas. *U. S. Geol. Survey Prof. Paper* **354-B**.

FRIPIAT, J. J. (1960) Application of infra-red spectroscopy to the study of clay minerals. *Bull. Groupe Francais Argiles*, **12**, 25–41.

HERMAN, R. AND R. J. RUBIN (1955) Influence of vibration-rotation interaction on line intensities in vibration-rotation bands of a rotating Morse oscillator. *Astrophys. Jour.* **121**, 533–540.

——— AND R. F. WALLIS (1955) Influence of vibration-rotation interaction on line intensities in vibration-rotation bands of diatomic molecules. *Jour. Chem. Phys.* **23**, 637–646.

HEXTER, R. M. (1961) Infrared spectrum of single crystals of LiOH, LiOD and LiOH ·LiOD. *Jour. Chem. Phys.* **34**, 941–947.

——— (1963) Comment on "Infrared absorption spectra of LiOH and LiOD." *Jour. Chem. Phys.* **38**, 1024–1025.

KLEINMAN, D. A. AND W. G. SPITZER (1962) Theory of the optical properties of quartz in the infrared. *Phys. Rev.* **125**, 16–30.

LIDIARD, A. B. (1954) Ionic conductivity of impure polar crystals. *Phys. Rev.* **94**, 29–37.

MATOSSI, F. (1949) Vibration frequencies and binding forces in some silicate groups (with references to his earlier work). *Jour. Chem. Phys.* **17**, 679–685.

MITRA, S. S. (1962) Vibration spectra of solids. *Solid State Physics*, **13**, 73.

NESBET, R. K. (1962) Approximate Hartree-Fock calculations for the HF molecule. *Jour. Chem. Phys.* **36**, 1518–1533.

PAULING, L. (1930) The structure of the micas and related minerals. The structure of the chlorites. *Proc. Nat. Acad. Sci.* **16**, 123–129, 578–582.

POLO, S. R. AND M. K. WILSON (1955) Infrared intensities in liquid and gas phases. *Jour. Chem. Phys.* **23**, 2376–2377.

PRIMA, A. M. (1957) The calculation of vibrational spectra of silicates. *Trudy Inst. Fiz. Mat., Akad. Nauk, Belorus. SSR*, **2**, 124–173.

RADOSLOVICH, E. W. (1960) The structure of muscovite. *Acta Cryst.* **13**, 919–932.

——— AND K. NORRISH (1962) The cell dimensions and symmetry of layer lattice silicates. *Am. Mineral.* **47**, 599–616.

SAKSENA, B. D. (1961) Infra-red absorption studies of some silicate structures (which also summarizes his earlier work). *Trans. Faraday Soc.* **57**, 242–258.

SERDYUCHENKO, D. P. (1948) Crystallochemical role of titanium in micas. *Dokl. Akad. Nauk. SSSR.* **59**, 739–742.

SERRATOSA, J. M. AND W. F. BRADLEY (1958a) Determination of the orientation of OH bond axes in layer silicates by infrared absorption. *Jour. Phys. Chem.* **62**, 1164–1167.

——— AND W. F. BRADLEY (1958b) Infra-red absorption of OH bonds in mica. *Nature*, **181**, 111.

———, A. HIDALGO AND J. M. VINAS (1962) Orientation of OH bonds in kaolinite. *Nature*, **195**, 486–487.

SKOW, M. L. (1960) Mineral facts and problems. *U. S. Bureau Mines Bull.* **585**, 534.

SPITZER, W. G. AND D. A. KLEINMAN (1961) Infrared lattice bands of quartz. *Phys. Rev.* **121**, 1324–1335.

STEINFINK, H. (1962) Crystal structure of a trioctahedral mica: phlogopite. *Am. Mineral.* **47**, 886–896.

STEPANOV, B. I. AND A. M. PRIMA (1958) The vibrational spectra of silicates. *Optika Spektr.* **5**, 15–22.

——— (1958) The vibrational spectra of silicates. *Optika Spektr.* **4**, 734–749.

STUBICAN, V. AND R. ROY (1961a) Isomorphous substitution and infra-red spectra of the layer lattice silicates. *Am. Mineral.* **46,** 32–51.

——— (1961b) A new approach to assignment of infra-red absorption bands in layer-structure silicates. *Zeit. Krist.* **115,** 200–214.

SUTHERLAND, G. B. B. M. (1955) Infra-red and X-ray analysis of crystal structure. *Nuovo Cimento Suppl. II Ser.* **10,** 635–641.

TARTE, P. (1961) Infra-red spectroscopic evidence of four-fold coordination of titanium in barium orthotitanate. *Nature,* **191,** 1002–1003.

TSUBOI, M. (1950) On the positions of the hydrogen atoms in the crystal structure of muscovite as revealed by the infra-red absorption study. *Bull. Chem. Soc.* (Japan), **23,** 83–88.

VAN DER MAREL, H. W. AND J. H. L. ZWIERS (1959) OH stretching bands of the kaolin minerals. *Silic. Indust.* **24,** 359–368.

VEDDER, W. AND R. S. MCDONALD (1963) Vibrations of the OH ions in muscovite. *Jour. Chem. Phys.* **38,** 1583–1590.

WICKERSHEIM, K. A. (1959) Infrared absorption spectrum of LiOH. *Jour. Chem. Phys.* **31,** 863–869.

——— AND R. A. LEFEVER (1962) Absorption spectra of ferric-ion containing oxides. *Jour. Chem. Phys.* **36,** 844–850.

*Mansucript received, November 4, 1963; accepted for publication, February 27, 1964*